

Study of spatial and temporal characteristics of L-band scintillations over the Indian low-latitude region and their possible effects on GPS navigation

P. V. S. Rama Rao, S. Gopi Krishna, K. Niranjana, and D. S. V. V. D. Prasad

Space Physics Laboratories, Department of Physics, Andhra University, Visakhapatnam 530 003, India

Received: 17 December 2005 – Revised: 8 March 2006 – Accepted: 6 April 2006 – Published: 3 July 2006

Abstract. The scintillation data (S4-index) at the L-band frequency of 1.575 GHz, recorded from a total of 18 GPS receivers installed at different locations in India under the GAGAN project, have provided us with a unique opportunity, for the first time in the Indian region, to make a simultaneous study of spatio-temporal and intensity characteristics of the trans-ionospheric scintillations during the 18-month, low sunspot activity (LSSA) period from January 2004 to July 2005. During this period, the occurrence of scintillations is found to be maximum around the pre-midnight hours of equinox months, with very little activity during the post-midnight hours. No significant scintillation activity is observed during the summer and winter months of the period of observation. The intensity (S4 index) of the scintillation activity is stronger around the equatorial ionization anomaly (EIA) region in the geographic latitude range of 15° to 25° N in the Indian region. These scintillations are often accompanied by the TEC depletions with durations ranging from 5 to 25 min and magnitudes from 5 to 15 TEC units which affect the positional accuracy of the GPS by 1 to 3 m. Further, during the intense scintillation events ($S4 > 0.45 \approx 10$ dB), the GPS receiver is found to lose its lock for a short duration of 1 to 4 min, increasing the error bounds effecting the integrity of the SBAS operation. During the present period of study, a total of 395 loss of lock events are observed in the Indian EIA region; this number is likely to increase during the high sunspot activity (HSSA) period, creating more adverse conditions for the trans-ionospheric communications and the GPS-based navigation systems.

Keywords. Ionosphere (Equatorial ionosphere; ionization mechanism; Ionospheric irregularities)

Correspondence to: P. V. S. Rama Rao
(palurirao@yahoo.com)

1 Introduction

The Global Positioning System (GPS) is a satellite-based navigation system, which provides good positional accuracy of the user at any point of the globe, and at any given time using the L-band frequencies of L1 (1575.42 MHz) and L2 (1227.60 MHz). The GPS positioning accuracies are subjected to various effects, like clock biases of the satellites and receivers, ionospheric and tropospheric delays, and receiver noise. Among these, the effects of accuracy degradation, due to group delay introduced by ionospheric total electron content (TEC) and ionospheric scintillations caused by small-scale density irregularities, are the most significant. Therefore, the standalone GPS is not suitable for certain navigation applications, like aircraft landing using a Category-I (CAT-I) precision approach. In the Indian region the augmenting of GPS is planned through a regional Satellite Based Augmentation System (SBAS), called GPS Aided Geo Augmented Navigation (GAGAN) from the Indian Space Research Organisation (ISRO) and Airport Authority of India (AAI).

Most of the Indian region encompasses the equatorial and low-latitude ionospheres. The morphology of the equatorial ionosphere is quite different from that of other latitudes because the magnetic field (\mathbf{B}) at the equatorial region is nearly parallel to the Earth's surface. During daytime, the E-region dynamo electric field (\mathbf{E}) is eastward. This field in the E-region and at off-equatorial latitudes maps along the magnetic field to F-region altitudes above the magnetic equator, resulting in $\mathbf{E} \times \mathbf{B}$ drift, which transports F-region plasma upward over the magnetic equator. The uplifted plasma over the equator then moves along magnetic field lines in response to gravity, diffusion, and pressure-gradient forces. As a result, the equatorial ionization anomaly is formed with reduced F-region ionization density at the magnetic equator and increased ionization at the two anomaly crests around $\pm 15^\circ$ in magnetic latitude to the north and south of the magnetic equator.

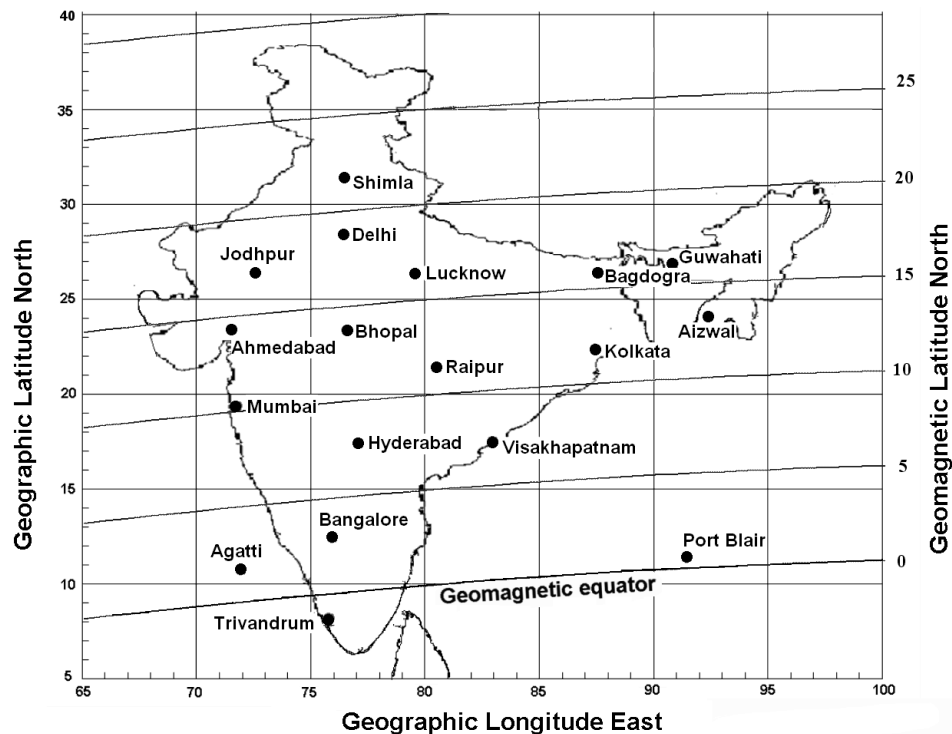


Fig. 1. Location of the GPS receiver installations in the Indian region.

It is known that near sunset, the dynamics of the equatorial ionosphere are dominated by the pre-reversal enhancement (PRE) (Woodman, 1976) of the vertical drift at the equator. During sunset, plasma densities and dynamo electric fields in the E-region decrease, and the anomaly begins to fade, and at this local time a dynamo electric field develops in the F-region. Polarization charges, set up by the conductivity gradients at the terminator, enhance the eastward electric field for about an hour after sunset. With the decreased ionization density in the E-region after sunset, vertical plasma density gradients form in the bottom side of the F-layer, resulting in the upward density gradients opposite in direction to the gravitational force. This configuration is Rayleigh-Taylor (RT) unstable and allows plasma density irregularities to generate (Kelley et al., 1981, 1986; Huang and Kelley 1996; Hysell, 2000). The eastward post-sunset electric fields enhance the R-T instability, while westward fields quench it. These irregularities can grow to become large ionospheric depletions, often called equatorial plasma bubbles, which are elongated along the magnetic flux tubes. The variability in the PRE may dictate the onset or inhibition of these instabilities (Basu et al., 1996; Hysell and Burcham, 1998; Fejer et al., 1999). The Indian region covers latitudes ranging from the magnetic equator to the northern anomaly crest and beyond, up to 27° N geomagnetic latitudes, and it is also known that scintillations are most severe at the locations around the anomaly crest where the electron density gradients are high (Aarons et al., 1981; Basu et al., 1988).

Small-scale irregularities in the electron content of the ionosphere, with spatial extents from a few metres to a few kilometres, can produce both refraction and diffraction effects on received GPS signals. The refraction changes the direction and speed of the propagation of an electromagnetic wave, and the diffraction gives rise to spatial fluctuations in the amplitude and phase of the received signal. The movement of the ionospheric irregularities relative to the signal path converts these spatial fluctuations, due to diffraction effects, into temporal fluctuations, which, due to the diffraction effects, are observed as scintillations in the GPS received signal (Wanninger, 1993). It was observed that during strong scintillation, deep amplitude fades or large phase fluctuations may cause signal disruptions in the receiver-satellite link (Skone et al., 2000; Kintner et al., 2001). Amplitude scintillations can be monitored by the time series of C/N_0 (signal-to-noise ratio) provided by the GPS output, and phase scintillations result from sudden changes in ionospheric refraction or from diffraction effects. The strong amplitude scintillation may cause the received signal power to drop below the receiver's threshold limit, and then a loss of lock is observed. The strong phase scintillation may cause a Doppler shift in frequency in the received signal carrier, exceeding the receiver's phase-lock-loop (PLL) bandwidth, resulting in a loss of phase lock of the receiver. It was observed that phase scintillations are always accompanied by at least moderate levels of amplitude scintillations (Doherty et al., 2004). Both the amplitude and phase scintillations increase

the root-mean-square (RMS) phase-tracking error in the output of the PLL; when the RMS jitter exceeds a threshold, loss of lock may occur even if the signal is above the threshold of the receiver (Knight and Finn, 1988; Conker et al., 2003). A decrease in the number of GPS signals locked by a user receiver can result in poor navigation accuracy. Moreover, loss of signal lock at SBAS monitoring stations can degrade the broadcast correction information.

This paper, for the first time, reports on scintillation characteristics observed at the L-band frequency of 1.575 GHz over the entire Indian region using eighteen-month data for the period from January 2004 to July 2005 from a network of eighteen GPS receiver stations in India. We present here the results on the spatio-temporal and intensity characteristics of the L-band scintillations (S_4 index), simultaneously measured by these receivers in the Indian region and the possible effects on GPS navigation.

2 Data and method of analysis

In the present study the amplitude scintillation (S_4 index) data at 1.575 Hz, recorded by the dual frequency GPS receivers installed at the 18 different locations in the Indian region under the Indian GAGAN programme during the eighteen-month period from January 2004 to July 2005, are used. The chain of receivers are installed such that they cover the Indian region from the magnetic equator to the equatorial anomaly crest and beyond, at a grid spacing of about $5^\circ \times 5^\circ$ in latitude and longitude, as depicted in Fig. 1. Here the longitudinal coverage of these stations vary from 72° E to 92° E, and the geographic latitudes vary from 8° to 32° N, covering a range of 1° S to 23° N magnetic latitudes.

The GSV 4004 Ionospheric Scintillation Monitor receivers (ISMs) are used to collect the TEC and scintillation data (Van Dierendonck et al., 1996). Each ISM can track up to 11 GPS C/A-code signals at the L1-frequency of 1.575 GHz. The data is collected at one-minute intervals, which do not include the 50-Hz sampled raw data, but did include statistical data for all satellites being tracked. The statistical data include parameters, like signal-to-noise ratio (C/N_0), standard deviation parameters of amplitude and phase, receiver lock time, and such other information for each satellite. The ISM calculates the standard deviation of the phase fluctuation (phase-sigma) and that of the signal intensity fluctuation normalized by its mean (S_4) from raw data sampled at a 50-Hz rate. The S_4 index is calculated from the normalized standard deviation of raw signal intensity (S_{4T}) and that of ambient noise ($S_{4,NO}$) by the formula $S_4 = \text{Sqrt}((S_{4T})^2 - (S_{4,NO})^2)$. It was specified that the phase parameters should be discarded for any lock time less than 240 s, to allow the detrending filter to reset, as it should be reinitialized whenever the lock is lost.

The scintillation index (S_4) and TEC data thus recorded, using the GPS receivers, are processed for each of the satel-

lite passes with an elevation mask angle greater than 40° , so that the effects of low elevation angles, such as tropospheric, water vapour scattering and multipath effects, are avoided. At low elevation angles high S_4 index values are observed (even during daytime hours), because the amplitude scintillation depends on the electron density deviations and on the thickness of the irregularity layer, both of which increase apparently at low elevation angles, causing stronger scintillations, and high S_4 index values due to multipath effects. The 40° mask angle may reduce the number of satellites available for the actual Satellite Based Augmentation System (SBAS) operation, but allows one to study the effects of ionospheric irregularities alone on the GPS navigation, limiting the tropospheric and multipath effects at the low elevation angles.

3 Results

3.1 L-band scintillations in the Indian region

In the recent years, with the increasing demand for the trans-ionospheric communications in the navigation of spaceborne vehicles, such as satellites, aircrafts and surface transportation systems, the study of ionospheric scintillations, particularly at the L-band frequencies (which is commonly used in these systems), has gained importance. It is well known that the scintillations are severe at the low-latitude and equatorial regions during the equinox months and during high sunspot activity (HSSA) periods (Aarons, 1982; Basu et al., 1988; Aarons, 1993). The Indian region includes the magnetic equator, the northern anomaly crest region and beyond up to 27° N geomagnetic latitudes. Therefore, the scintillation activity is severe for more than half of the area (equatorial ionization anomaly region) in the Indian Flight Information Region (FIR), as may be seen from Fig. 1.

Therefore, with a view to examine the nature of the occurrence of scintillations over the entire Indian region at any give point in time, plots of the S_4 index, as a function of local time (from 18:00 to 06:00 LT), are made for all 18 stations for each day from all the available satellite passes. In Fig. 2, the day-to-day occurrence of scintillations during the month of March 2004 is presented for four typical stations, namely, Trivandrum (8.4° N geographic latitude, 0.47° S geomagnetic latitude), Waltair (17.7° N G., 8.22° N G.M), Raipur (21.1° N G., 12.78° N G.M) and Jodhpur (26.2° N G., 17.6° N G.M), representing the four different latitude zones in the Indian sector. Trivandrum is an equatorial station, Waltair is a sub-tropical station situated at the inner edge of the equatorial ionization anomaly (EIA), Raipur is a station situated in the crest region of the anomaly, whereas Jodhpur is situated beyond the anomaly crest region. The power levels of the scintillation recorded (S_4 index) presented in Fig. 2 are divided into three categories, namely weak (3 to 6 dB, i.e., $S_4=0.17$ to 0.3), moderate (6 to 10 dB,

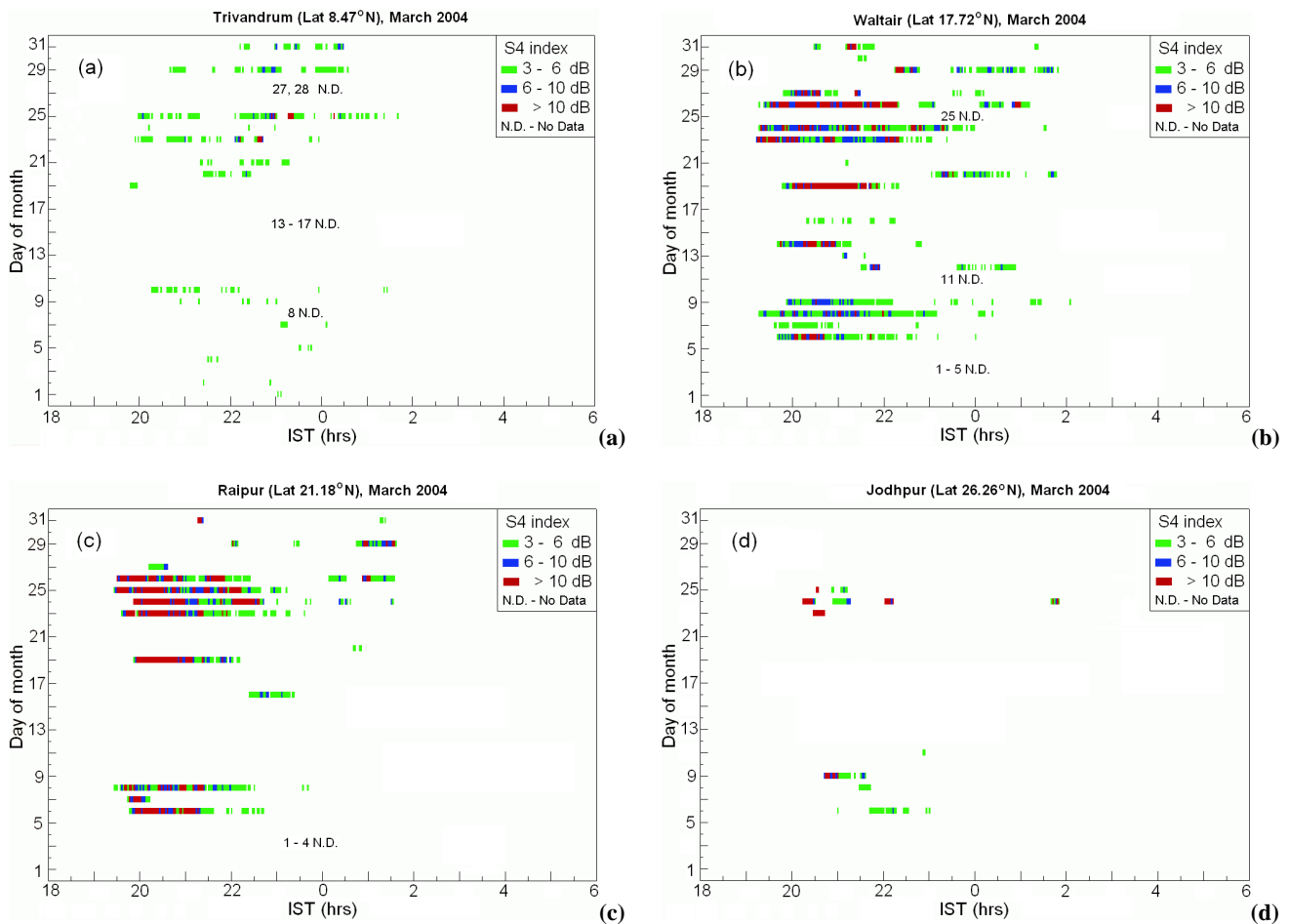


Fig. 2. Day-to-day occurrence of scintillations at different power levels during the month of March 2004 at four typical Indian latitudes representing an (a) equatorial station (Trivandrum), (b) low-latitude station (Waltair), (c) anomaly crest station (Raipur), (d) station beyond the anomaly crest (Jodhpur).

i.e., $S4=0.3$ to 0.45) and strong ($S4 > 10$ dB) scintillations, respectively.

It may be seen from Fig. 2a, which shows the scintillation occurrence at the equatorial station, Trivandrum, that the occurrence of weak scintillations (3 to 6 dB) are greater, with practically no occurrence of strong (> 10 dB) scintillations. At Waltair, a station situated at the inner edge of the equatorial anomaly crest (Fig. 2b), the occurrence of scintillations at all three power levels is high. At Raipur (Fig. 2c), a station situated at the crest of the anomaly, the occurrence of a strong scintillation is highest. At Jodhpur (Fig. 2d), a station situated beyond the anomaly crest region, the scintillation activity has considerably decreased to a minimum. The set of these four figures clearly indicates that strong (> 10 dB) scintillations occur at and around the EIA region, owing to the presence of short scale length (\sim few hundred metres) irregularities and high ambient electron densities accompanied by large electron density gradients, even during the low sunspot activity (LSSA) period of March 2004. On the other

hand, it may be noticed that for the occurrence of weak scintillations over the magnetic equator, Trivandrum is maximum compared to the occurrence of weak scintillations at the crest region. Here it may be mentioned that due to the geographic shape of India, the number of GPS receiver stations are less, limiting the spatial coverage (added to that lack of data from 13 to 17 March 2004), around the equatorial region compared to the crest region. Hence, the weak scintillation activity is not prominently visible to the extent expected in Fig. 2a. The occurrence of weak scintillations is due to the presence of large-scale size irregularities, low ambient electron densities and low electron density gradients at the equator during the LSSA periods. At the anomaly crest regions, the accumulated F-region ionization, transported from the equator, is high, resulting in high electron density gradients and small-scale irregularities, giving rise to the generation of strong scintillations at the L-band frequency of 1.5 GHz.

In Figs. 3a–c the percentage occurrence of scintillations as contour diagrams is presented at the three different power

ranges, over the entire country, with a view to study the latitudinal variation as a function of local time for the equinoxial month of March 2004. It may be seen from Fig. 3a that the percentage occurrence of weak (3 to 6 dB) scintillations is maximum (58%), with peak occurrence around 21:00 LT at 17° N geographic latitude. The percentage occurrence of moderate (6 to 10 dB) scintillations (Fig. 3b) is relatively low, with peak occurrence (44%) confined to 21:00 LT at latitudes of 15° to 20° N. Strong (> 10 dB) scintillations are presented in Fig. 3c, where the percentage occurrence is lowest (37%) compared to weak and moderate scintillations. The peak occurrence of strong scintillations during this month (March 2004) is confined to 17° N geographic latitude and to the local time of 21:00. From Figs. 2 and 3 it may be noticed that most of the L-band scintillations in the Indian region occur during the pre-midnight period of 19:00–24:00 LT with a scanty occurrence during the post-midnight hours.

The constellation of orbiting GPS satellites radiating signals at the L-band frequency of 1.575 GHz has given a unique opportunity to measure the S4-index simultaneously and continuously over the entire Indian region using the GPS network of receivers installed, almost evenly, at different places in India. The data of the S4 index thus collected has been categorized into three different power levels, namely all those scintillations greater than 3 dB ($S4=0.17$), those greater than 6 dB ($S4=0.3$) and all those greater than 10 dB ($S4=0.45$). The monthly mean percentage occurrences of these scintillations for the 18-month period (January 2004 to July 2005) are computed, and their temporal (month to month) and spatial (latitudinal) variations are presented in Figs. 4a–c, respectively, representing the three different power levels. It is striking to observe from this figure that the occurrence of scintillations is maximum during the equinox months. From Fig. 4a, which corresponds to the occurrence of scintillations with all power levels >3 dB, it may be noticed that the maximum percentage occurrence is seen around the vernal equinox months of March and April of 2004, and February and March of 2005, at all latitudes up to 20° N. The next maximum with reduced intensity occurs around the autumn equinox months of September and October 2004. There is practically no scintillation activity during the winter and summer months of the low sunspot years of 2004 and 2005 at the L-band frequency of 1.575 GHz. The equinoxial maxima are explained on the basis of the alignment of the solar terminator with the magnetic meridian in both the hemispheres (Tsunoda, 1985). Over the sunlit hemisphere, the E-region ionization short circuits the polarization electric fields, developed in the F-region during the evolution phase of the ESF irregularities. During the equinox, the solar terminator aligns closely with the magnetic meridian, thereby simultaneously decreasing the conductivity of the E-regions that are magnetically conjugate to the F-layer, through which currents flowing along the geomagnetic field lines connect the F-region to the E-regions on either side of the equator (which acts as a short circuit over the sunlit hemisphere). This alignment

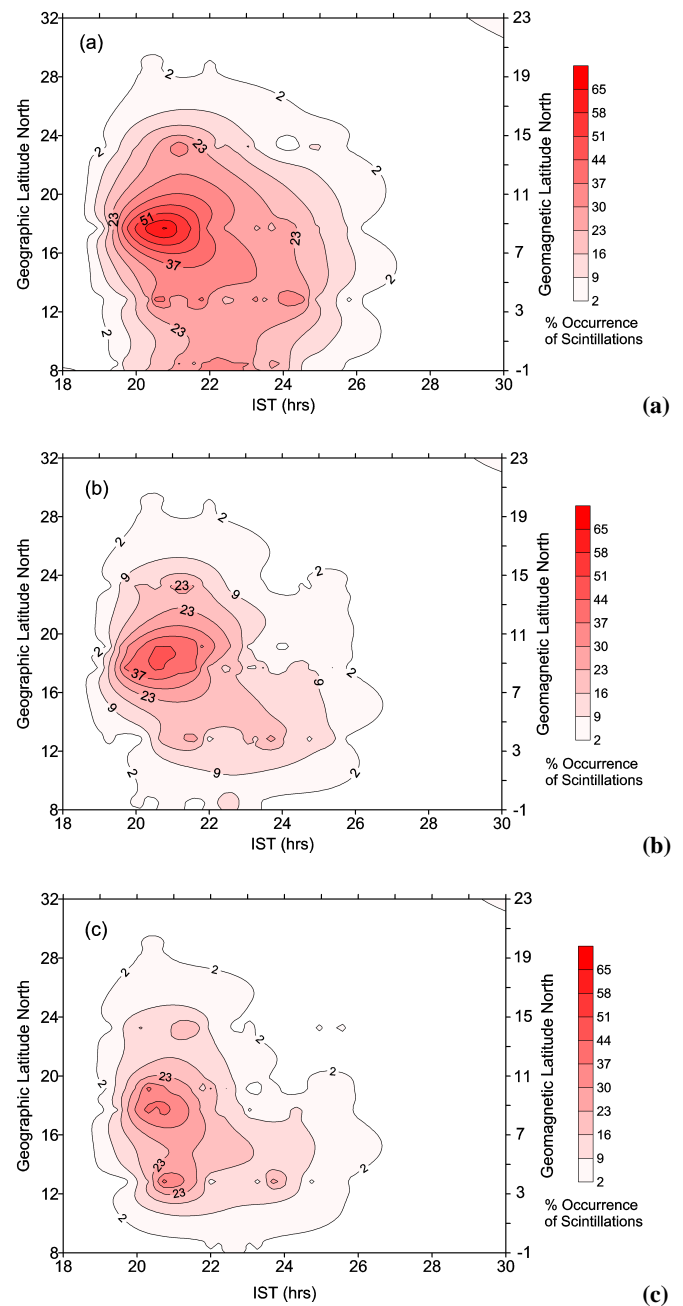


Fig. 3. Temporal and spatial variation of the percentage occurrence of scintillation activity as a function of their intensity over all the Indian stations as observed from GPS S4 index data for the equinox month of March 2004 at power levels of (a) 3 to 6 dB, (b) 6 to 10 dB and (c) > 10 dB.

causes the decrease in E-region conductivity, which opens or releases the F-region dynamo electric field, which, in turn, produces the $E \times B$ upward drift of the equatorial F-layer, creating favorable conditions for the generation of plasma irregularities during the equinox months, as seen above.

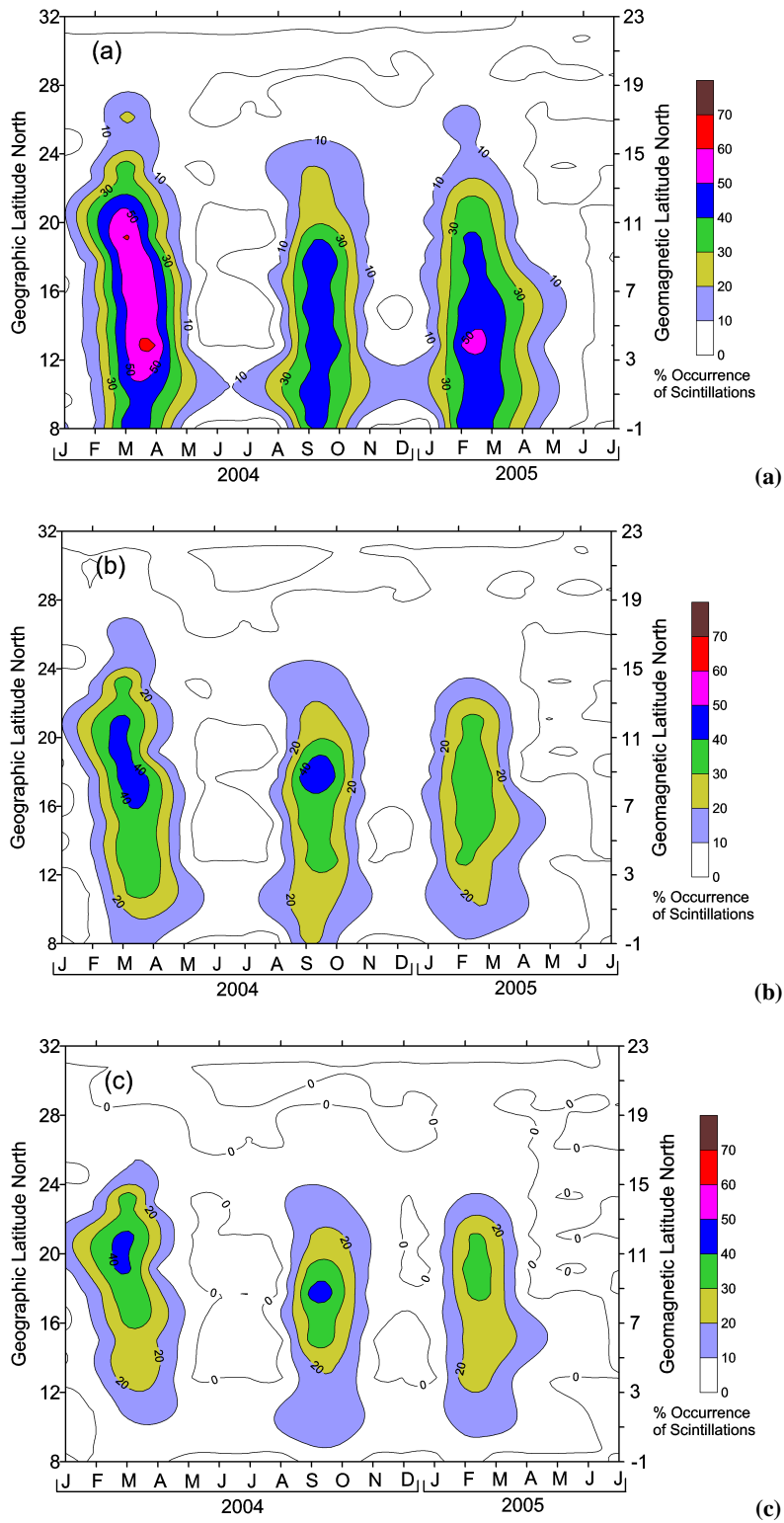


Fig. 4. Temporal and spatial variations in the occurrence of scintillations during the low sunspot activity years of 2004 and 2005 at different power levels of (a) >3 dB, (b) >6 dB, (c) >10 dB.

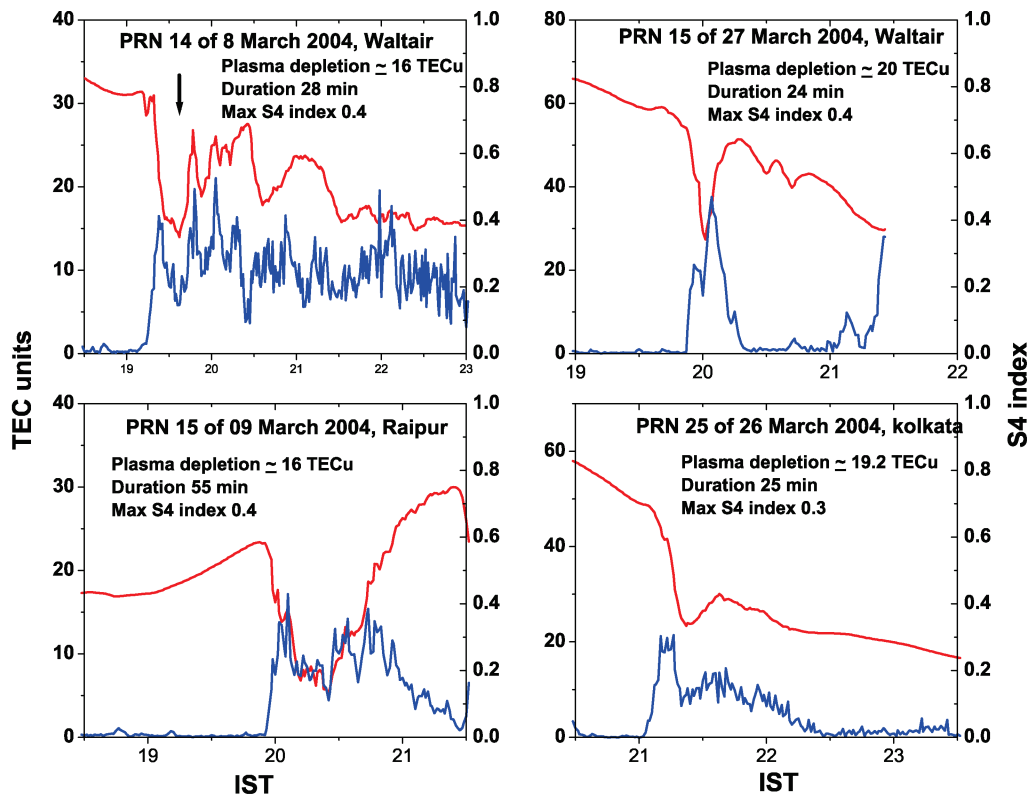


Fig. 5. Some examples of scintillations (S4 index) associated with TEC depletions observed in the GPS data at four typical Indian stations.

Further, it is interesting to note from Fig. 4a that, even though the monthly mean sunspot number of the equinox month of March 2005 ($R_z=24.8$) is lower than that of the winter month of November 2004 ($R_z=43.7$), the scintillation activity is much higher (45%) in March 2005 than in November 2004, where there is practically no scintillation occurrence, clearly suggesting that the seasonal dependence of scintillation occurrence dominates over the sunspot number dependency during the descending phase of the sunspot number.

It is known that the occurrence of scintillations in the equatorial regions increases with the increase of sunspot activity, with maximization during the HSSA period. Also, the occurrence of scintillations is modulated by the seasonal effect, with maximum occurrences during the equinox months followed by winter and a minimum occurrence during summer months. During the moderate to high sunspot activity periods, the seasonal modulation in the occurrence pattern of scintillations is significant (DasGupta et al., 1983; Rama Rao et al., 2006). However, during relatively low sunspot number periods, such as 2004–2005, and during the descending phase of the sunspot number, the seasonal control on the scintillation activity is predominantly perceptible over the sunspot number dependence, as may be seen from Fig. 4a. Further, the occurrence of scintillations greater than 6 dB (Fig. 4b) also shows similar features, but with a reduced per-

centage of occurrences and with the peak occurrences limited to reduced latitudinal width. When we look at the percentage occurrence of scintillations greater than 10 dB (Fig. 4c), which are of serious concern in transionospheric communication at the L-band frequencies, it may be seen that the occurrences are relatively reduced and are mostly confined to a lesser latitudinal belt around 20° N during the vernal equinox and to 18° N in the autumn equinox. Thus, it may be concluded that strong (>10 dB) scintillations do occur, particularly during the equinox months in the low-latitude sectors, such as in India, even during the LSSA period.

3.2 Characteristics of TEC depletions/bubbles

The ordinary source of equatorial electrodynamics is the thermospheric dynamo that powers the equatorial electrojet (Haerendel and Eccles, 1992; Eccles, 1998). During the daytime, at ionospheric F-region altitudes, the vertical polarization electric fields, setup by the dynamo currents that are created by thermospheric winds, are short circuited through the conducting sunlit E-layer to the north and south of the magnetic equator. However, after sunset, the eastward electric field attributed to the F-region dynamo is enhanced following the decrease in the E-region conductivity; this field induces the upward $E \times B$ drift. This pre-reversal enhancement of the eastward electric field raises the F-layer at the

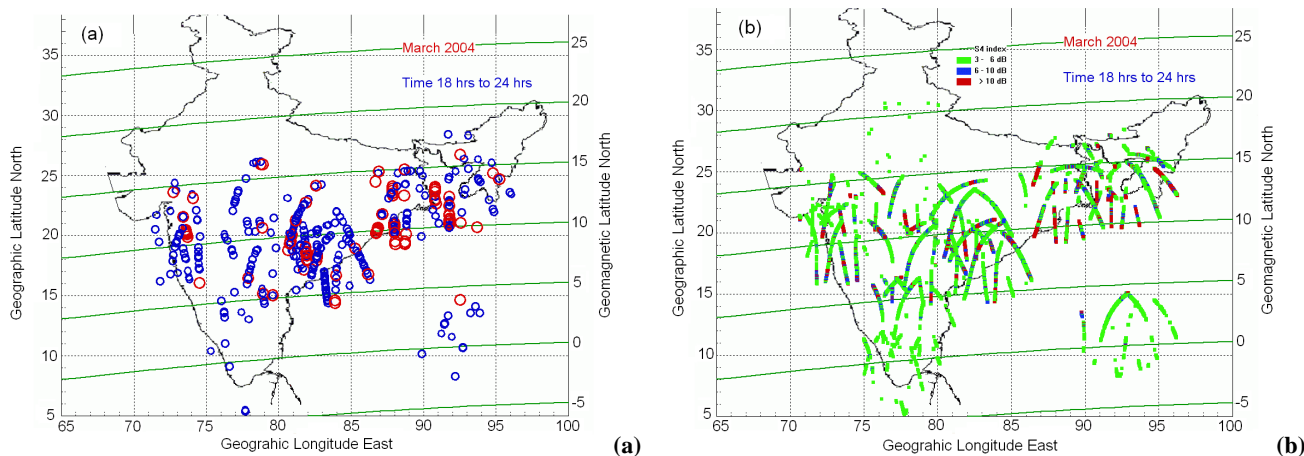


Fig. 6. Occurrence of L-band scintillations associated with TEC depletions (bubbles) and loss of lock events during the month of March 2004: (a) bubbles (blue circles) and loss of locks of the GPS receivers (red circles) and (b) the scintillations at three different power ranges of 3 to 6 dB (Green), 6 to 10 dB (Blue) and > 10 dB (Red).

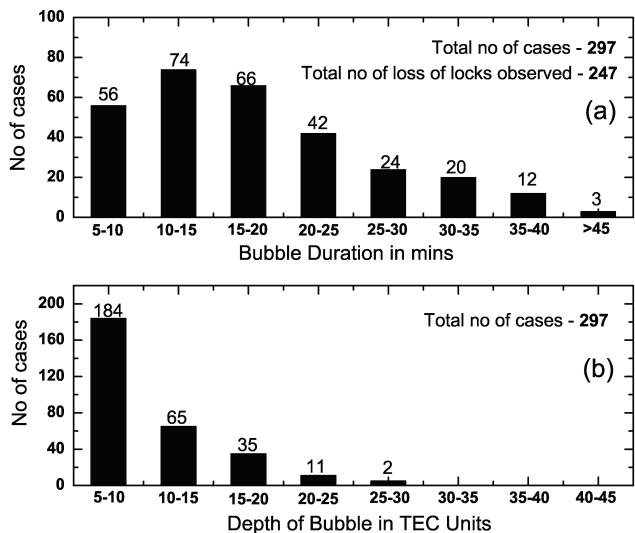


Fig. 7. Histograms showing the duration (a) and intensity (b) of the TEC depletions observed over the Indian region for the month of March 2004.

magnetic equator to high altitudes, where the recombination rates are low and the conditions are favorable for generation of instabilities on the bottomside of the F-layer. Also, sharp upward density gradients are developed after sunset due to the rapid recombination of electrons and ions. The nonlinear development of these instabilities leads to the formation of the plasma depleted bubbles (Woodman and La Hoz, 1976; Kelley, 1989). The polarization electric field within the bubbles is higher and as a result, the bubbles rise to the topside at a velocity higher than the ambient plasma drift (Anderson and Haerendal, 1979). The steep gradients on the edges of the depletions generate the small-scale irregularities as the

bubbles rise to great heights (Costa and Kelley, 1978); these are widely recognized as plumes on radar backscatter maps (Woodman and La Hoz, 1976), extending along the magnetic field line to the anomaly crests of about $\pm 15^\circ$ magnetic latitudes. In the present study, the scintillations observed with the GPS L-band frequency of 1.575 GHz, around the anomaly crest regions, are often found to be associated with the plasma bubbles, which are detected as TEC depletions in the GPS TEC data.

It is known that the occurrence characteristics of the plasma depletions depend strongly on season and longitude (Aarons, 1993; Huang et al., 2001). When the depleted ionospheric plasma comes into the line-of-sight between the GPS satellite and the receiver, the TEC decreases and is observed as a depletion in the diurnal variation of TEC. It is also found that the presence of TEC depletions are often accompanied by an amplitude scintillation of high intensity and fading rates, particularly, during the pre-midnight period, where there may be a series of bubbles occurring within a single scintillation patch. Similar features in the occurrence of bubbles and scintillations are also reported by Yeh et al. (1979), DasGupta et al. (1983).

Plasma depletions are of particular importance when they extend to the latitudes of the anomaly crest region; where these bubbles intersect the highest levels of electron density, so that transionospheric radio frequency propagation through this intersection undergoes the highest disruptive levels of scintillation, both in amplitude and in phase levels, which are the highest during solar maximum (Klobuchar et al., 1991). In the present study, several depletions in TEC are detected which are often accompanied by the presence of intense scintillations, as seen from the increase in the S4 index measured by the GPS L1 signal. This can be seen from the typical examples of depletions in TEC, shown in Fig. 5. It is

Table 1. Number of depletions observed from each station (latitudes of each station tabulated) for every month during the period from January 2004 to February 2005. The monthly mean sunspot numbers are also shown under each of the months.

Station Geographic Latitude	Number of depletions observed for the months during Jan 2004 to Jul 2005																		
	Months with Rz	Jan 37.3	Feb 45.8	Mar 49.1	Apr 39.3	May 41.5	Jun 43.2	Jul 51.1	Aug 40.9	Sep 27.7	Oct 48.0	Nov 43.5	Dec 17.9	Jan 31.3	Feb 29.2	Mar 24.5	Apr 24.4	May 42.6	Jun 39.6
8.47	--	0	1	10	0	0	0	0	5	2	0	0	0	3	0	0	0	0	0
10.83	--	--	--	--	--	--	--	--	10	4	1	0	0	8	14	0	0	0	0
11.67	--	--	10	17	0	0	--	2	3	--	--	--	--	--	6	3	1	0	0
12.95	0	1	8	21	0	0	0	0	29	19	0	1	0	15	8	2	0	0	0
17.44	--	--	32	9	0	0	0	0	37	35	0	0	0	28	15	2	0	0	0
17.72	--	--	55	15	0	0	0	3	20	20	0	2	0	30	8	0	0	0	0
19.09	--	--	43	6	0	0	0	0	22	17	0	0	2	23	7	1	2	0	0
21.18	--	--	39	5	0	0	1	0	16	16	0	0	0	21	7	0	0	0	0
22.64	0	2	45	4	0	0	0	0	23	2	0	0	0	11	3	0	0	0	0
23.06	--	0	10	0	0	0	0	0	0	7	0	0	0	8	1	0	0	0	0
23.28	0	1	12	0	0	0	0	0	7	5	0	0	0	2	1	0	0	0	0
23.83	--	3	31	2	0	0	4	1	4	2	0	0	0	12	2	0	0	0	0
26.12	0	0	5	0	0	0	0	0	0	0	0	0	0	3	0	0	0	0	0
26.26	0	2	1	0	0	0	0	0	0	0	0	0	0	0	0	0	0	0	0
26.68	--	0	5	0	0	0	3	0	1	0	0	0	0	0	0	0	0	0	0
26.76	--	--	0	0	0	0	0	0	0	0	0	0	0	0	0	0	0	0	0
28.58	2	0	0	0	0	0	0	0	0	0	0	0	0	0	0	0	0	0	0
31.09	--	--	--	--	--	0	0	0	0	0	0	0	0	0	0	0	0	0	0
Total no of depletions	2	9	297	89	0	0	8	6	177	129	1	3	2	164	72	8	3	0	0

observed that when the plasma depletion is detected in the vertical TEC data derived from the satellite pass, the spatial gradients of TEC ($\Delta\text{TEC}/\Delta\text{Latitude}$, ratio of change in TEC to the change in latitude) at the edge of the bubbles are found to vary from 10 to 40. These density gradients give rise to favorable conditions for the generation of small-scale irregularities that effect the L-band frequencies. However, in the present study, strong scintillations ($S4 \geq 0.45 \approx 10 \text{ dB}$) are found to occur at and around the equatorial ionization anomaly region, if the gradients are greater than 15. Further, these gradients are found to vary from 15 to 40 closer ($\pm 5^\circ$) to the anomaly crest region. As the plasma depletions extend in latitude to the crest regions, the strong scintillations, which are associated with small-scale irregularities, contribute to the degradation of the positional accuracies in the satellite navigational systems, such as GPS. In Figs. 6a and b, a typical example is shown in the nocturnal occurrence pattern of depletions and associated scintillations (S4 index), respectively, as a function of latitude in the Indian region, for the month of March 2004. The S4 index and the TEC depletions detected from the GPS signals are plotted in these figures spatially, where the blue circles in Fig. 6a indicate the plasma depletions, and the red circles show loss of lock events in the phase channel of the GPS receiver, which will be discussed in a later section of this paper.

It may be seen from Fig. 6a that most of the depletions seen are confined to the anomaly crest region of geomagnetic latitudes ranging from 5° to 15° N (i.e. 15° to 25° N geographic latitudes). The same belt of latitudes also shows the presence of intense ($S4 \text{ index} > 0.45$) scintillation activity, as may be seen from Fig. 6b. The scintillations are moderate to weak at latitudes closer to the equator, because of the presence of low electron density and the absence of the short-scale length irregularities, which do not significantly affect the radio signals at L-band frequencies. At the anomaly crest region, because of increased electron densities and the presence of large gradients, the generation of small-scale irregularities is relatively high, which contributes to the occurrence of strong scintillations that severely effect the L-band signals.

It is also interesting to note that the TEC depletions and the strong scintillation events are aligned more to the geomagnetic latitudes, showing that the geomagnetic field control exists on these events. The population of scintillation events with a high S4 index is more in the inner edge of the anomaly crest compared to that at the outer edge, where the TEC falls more sharply towards the mid latitudes than towards the equator.

The length of the durations of the plasma depletions and the depth of their amplitudes determine the effect on the GPS-based navigation systems. In the equinox month of March 2004 alone, a maximum number (297) of depletions

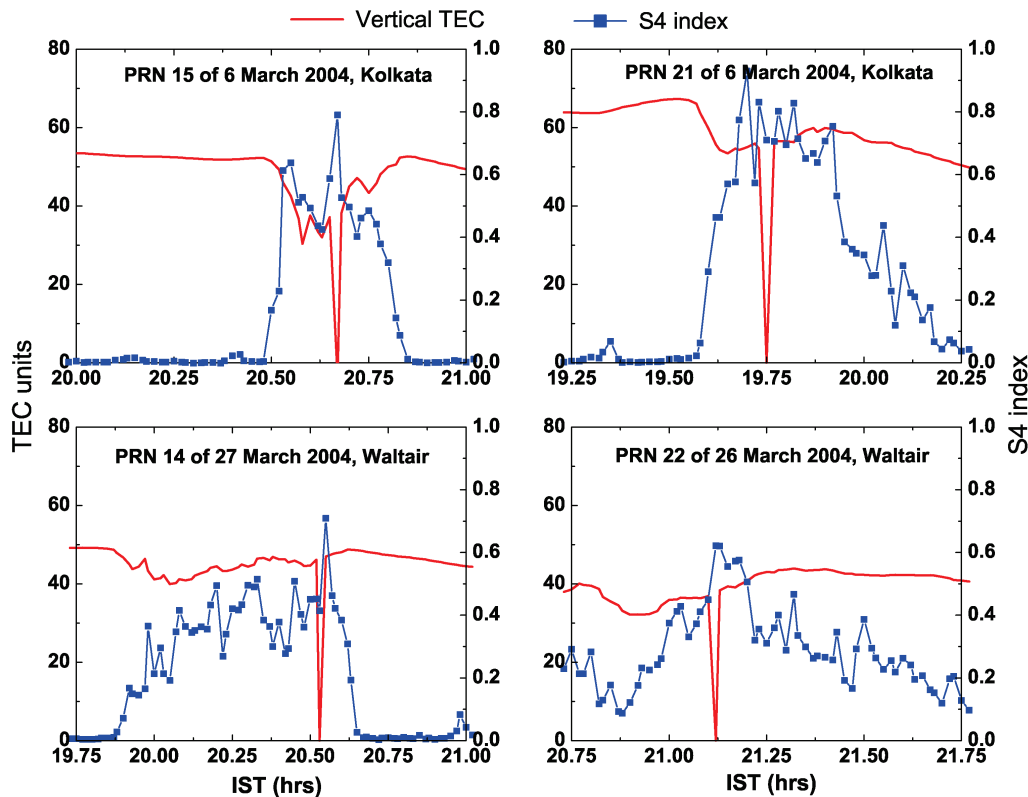


Fig. 8. Typical examples of scintillation activity showing the values of the S4 index exceeding 0.45, causing a loss of lock in the GPS receivers.

are detected from all the Indian stations. The TEC depletions observed during this month are categorized into different ranges of durations and amplitudes in TEC units, and presented as histograms in Figs. 7a and b, respectively. It is observed from these histograms that the most probable bubble durations vary from 5 to 25 min (Fig. 7a) and the most probable depth of depletions vary from 5 to 15 TEC units (Fig. 7b). It is known that the ionosphere causes a group delay of 0.162 m per one TEC unit (10^{16} ele/m²) at the GPS L1 frequency of 1.575 GHz (Warnant, 1997; Klobuchar et al., 1993), and thus in the present case, the depletion amplitudes of 5 to 15 TEC units introduce range errors of the order of 1 to 3 m.

In Table 1 the number of depletion events observed from all 18 Indian stations is listed by month during the 18-month period from January 2004 to July 2005. It can be seen from the table that a total number of 971 depletion events are detected over the entire Indian region during the 18-month period. Further, it may also be seen that a maximum number of depletions occur in the equinox months of March, April, September and October of 2004, and February and March of 2005, and at stations in the geographic latitude range of 13° to 24° N. Also, it is seen from the table that the latitude range in the occurrence of depletions is slightly higher in the vernal equinox months of March and April, compared to the

autumnal equinox months of September and October 2004. Further, the occurrence of depletions during February and March of 2005 is smaller compared to those during the corresponding months of the year 2004, owing to the decrease in the monthly average sunspot number (R_z) from 49 in March 2004 to 25 in March 2005.

Further, at the anomaly crest region, during the post-sunset hours, when strong scintillation ($S4 > 0.45$) activity is present, the TEC has shown the presence of strong depletions, with amplitudes varying from 10 to 30 TEC units, which correspond to a range error of 1.62 to 4.87 m in the GPS positional accuracies. Hence, the duration of the depletion and depth of amplitude in TEC play an important role in introducing errors in the range correction from the SBAS signals derived from the reference stations. Therefore, the region with a geographic latitude range of 15° to 25° N in the Indian sector, which is almost 50% of the SBAS area in India, is expected to be frequently affected by strong scintillations and depletions, particularly during equinox months, even during the LSSA periods (2004–2005). The range of latitudes or the FIR region which is likely to be affected by the scintillations could be expected to increase significantly with the increase in solar activity.

Table 2. Number of loss of lock events observed from each station (latitudes of each station tabulated) for every month during the period from January 2004 to February 2005. The monthly mean sunspot numbers are also shown under each of the months.

Station Geographic Latitude	Number of Loss of locks observed for the months during Jan 2004 to Jul 2005																		
	Months with Rz	Jan 37.3	Feb 45.8	Mar 49.1	Apr 39.3	May 41.5	Jun 43.2	Jul 51.1	Aug 40.9	Sep 27.7	Oct 48.0	Nov 43.5	Dec 17.9	Jan 31.3	Feb 29.2	Mar 24.5	Apr 24.4	May 42.6	Jun 39.6
8.47	0	0	1	10	0	0	0	0	5	2	0	0	0	3	0	0	0	0	0
10.83	--	--	--	--	--	--	--	--	10	4	0	0	0	8	14	0	0	0	0
11.67	--	--	10	17	0	0	0	2	3	--	--	--	--	--	6	0	0	0	0
12.95	0	0	8	21	0	0	0	0	29	19	0	0	0	15	8	0	0	0	0
17.44	--	--	32	9	0	0	0	0	37	35	0	0	0	28	15	0	0	0	0
17.72	--	--	55	15	0	0	0	3	22	20	0	0	0	30	8	0	0	0	0
19.09	--	--	43	6	0	0	0	0	20	17	0	0	0	23	7	0	0	0	0
21.18	--	--	39	5	0	0	1	0	16	16	0	0	0	21	7	0	0	0	0
22.64	0	1	45	4	0	0	0	0	23	2	0	0	0	11	3	0	0	0	0
23.06	--	0	10	0	0	0	0	0	0	7	0	0	0	8	1	0	0	0	0
23.28	0	1	12	0	0	0	0	0	7	5	0	0	0	2	1	0	0	0	0
23.83	--	2	31	2	0	0	0	1	4	2	0	0	0	12	2	0	0	0	0
26.12	0	1	5	0	0	0	0	0	0	0	0	0	0	3	0	0	0	0	0
26.26	0	1	1	0	0	0	0	0	0	0	0	0	0	0	0	0	0	0	0
26.68	--	0	5	0	0	0	0	0	1	0	0	0	0	0	0	0	0	0	0
26.76	--	0	0	0	0	0	0	0	0	0	0	0	0	0	0	0	0	0	0
28.58	1	0	0	0	0	0	0	0	0	0	0	0	0	0	0	0	0	0	0
31.09	--	0	0	0	0	0	0	0	0	0	0	0	0	0	0	0	0	0	0
Total loss of locks	1	6	195	30	0	0	1	0	65	39	0	0	0	36	22	0	0	0	0

3.3 Loss of lock of the GPS receivers

GPS receiver tracking performance becomes degraded in the presence of scintillation effects. Rapid phase variations cause a doppler shift in the GPS signal, which may exceed the bandwidth of the phase lock loop (PLL), resulting in a loss of phase lock (Leick, 1995). Additionally, amplitude fades can cause the signal-to-noise-ratio (SNR) to drop below the receiver threshold level, resulting in loss of code lock. These effects have a larger impact on tracking loops employing codeless and semicodeless technologies, versus full code correlation. In particular, codeless and semicodeless tracking loops experience losses of 27–30 dB and 14–17 dB, respectively, with respect to full code correlation, and are therefore more susceptible to the effects of amplitude fading (Leick, 1995). The L2 phase locked loop (PLL) also employs a narrower bandwidth (≈ 1 Hz, compared to ≈ 15 Hz for L1) to eliminate excess noise, and is more susceptible to loss of lock due to phase scintillations. These effects, therefore, are of significant concern for users who require dual frequency data for estimation of ionospheric effects, or resolution of widelane ambiguities. Investigations of GPS receiver performance recently conducted by Knight et al. (1999), using an array of eight GPS receivers in the equatorial region, have shown that on some occasions L2 phase observations were corrupted up to 27% of the time, and a loss of L2 code lock

was often observed. L1 tracking performance was degraded to a lesser extent. The results of such studies depend not only on the magnitude of scintillation activity, but also on the receiver tracking capabilities which can vary widely between different manufacturers and models.

In Fig. 8 some typical samples of loss of locks detected in the GPS receiver TEC data are shown during times of severe scintillations. It can be noticed from this figure that loss of locks are observed whenever the S4 index exceeds a 10 dB ($S4 > 0.45$) power level. The receiver PLL recovers from the loss of lock within a short duration of about 1 to 4 min. It was also observed that the receiver loses its lock more than once when the scintillation activity is severe, particularly at the anomaly crest regions, and also if the satellite is at a low elevation angle.

It may be recalled that in Fig. 6a, the spatial distribution in the occurrence of depletions/bubbles can be seen, where the loss of lock events (red circles) of the receivers are also plotted, in order to examine the spatial distribution of these events during the typical month of March 2004. It may also be seen from this figure that the loss of locks occur in the same geographic latitude range of 15° to 25° N, similar to those of bubbles and strong scintillations. In Fig. 6b, the corresponding S4 index data for the month of March 2004 is shown as colour coded dots (red) for $S4 \text{ index} > 0.45$, where it is observed that there is a good correspondence between

the occurrence of an S4 index greater than 0.45 and the loss of lock events. From a close examination of the GPS data with the help of an in-house developed software, it is noticed that whenever the L-band scintillation activity (S4) exceeds 0.45 or a 10 dB power level, the receiver loses its lock for a duration of about 1 to 4 min. The GPS receiver loss of locks thus detected from all the Indian stations during the 18 months of data are listed as a function of latitude in Table 2. From this table it is seen that the GPS receivers are subjected to a loss of locks mostly during the equinox months of March, April, September and October of 2004, and February and March of 2005, where the S4 index often exceeded 0.45 (10 dB). Further, it may also be seen that these loss of locks occur in the regions of strong scintillation (10 dB and above) occurrences, as may be seen from Fig. 4c. During this period, a maximum number of loss of lock events are observed only during equinox months. As many as 247 loss of lock events are observed during the month of March 2004 (Fig. 7) alone, from all the GPS receivers located in the Indian region. The geographic latitude zone of 15° to 25° N is identified to be the most affected region in the equinox months during this period. There are practically no loss of lock events in the post-midnight hours and during the summer and winter months. The latitude range, as well as the number of loss of lock events, may increase significantly during the ascending phase of the sunspot activity.

The plasma depletions that might have been detected simultaneously by two or three GPS satellite signals which have the line of sight through the same depletion region are not separately accounted for in this preliminary study, as the emphasis is on the number of available satellite PRNs which are affected by these plasma depletions for the SBAS operation. Therefore, the number of TEC depletions detected here may give rise to a larger number than the actual number of plasma bubbles which existed in that region at that point of time, and each of the detected bubbles may have a different duration and magnitude depending on their intersection direction and duration with that particular plasma depletion. This may be one of the reasons why the number of TEC depletions observed is much greater (971) than the number of loss of lock events (345) detected. Further, all the plasma depletions may not intersect high density TEC regions in order to have enough gradients on the edges of the depleted regions which can generate the small-scale length irregularities to produce intense scintillations (>10 dB), which could lower the GPS signal power below the threshold level (due to strong amplitude scintillation) or could cause rapid phase changes in the received signal which results in a loss of lock of the receiver. In addition, no loss of lock events are detected without the presence of a TEC depletion and intense scintillation activity (S4>0.45).

3.4 Summary of results and discussion

The scintillation index (S4) data at the L-band frequency of 1.575 GHz, recorded simultaneously from the GPS receivers installed at 18 different locations (nearly at a spacing of 5°×5° grid) under the ISRO-GAGAN programme in the Indian region, has given us a unique opportunity, for the first time, to study the spatio-temporal and intensity characteristics of the ionospheric scintillations during the 18-month period from January 2004 to July 2005. The results of the study reveal the following characteristic features in the occurrence of the L-band scintillations in the Indian equatorial and low-latitude region.

3.4.1 L-band scintillation characteristics

1. The percentage occurrence of L-band scintillations is maximum during the post-sunset to midnight hours, with very little activity during the post-midnight hours in the current LSSA period of 2004–2005.
2. The percentage occurrence of weak (3 to 6 dB) scintillations is maximum at the equatorial region, owing to the presence of low ambient electron densities and low gradients accompanied by the presence of large-scale length irregularities at the equator during the LSSA conditions in the years 2004 and 2005.
3. The intensity of scintillation (S4 index) is maximum (>10 dB) around the anomaly crest region because of the presence of high electron densities and large gradients accompanied by the presence of small-scale irregularities at the anomaly crest regions.
4. Scintillations are found to occur mostly during the equinox months, with practically no activity during the summer and winter months of the LSSA period of 2004–2005.
5. The occurrence of strong scintillations is mostly confined to 15° to 25° N geographic latitudes i.e. 5° to 15° N geomagnetic latitudes in the Indian region.
6. It is found that the equinoxial feature dominates in the occurrence of scintillations, giving rise to higher occurrences in the equinox months of March, April of 2004 and 2005, with practically no activity during winter and summer months.

3.4.2 Characteristics of electron density depletions/bubbles observed in the GPS TEC data

1. A significant number of TEC depletions are found to occur during the post-sunset hours, often accompanied by the occurrence of scintillations at the L-band frequency of 1.575 GHz of the GPS L1 signal.

2. The occurrence of these bubbles is also found to be maximum during the equinox months, peaking around the equatorial ionization anomaly crest region of 15° to 25° geographic latitudes.
3. The most probable bubble durations vary from 5 to 25 minutes and their amplitudes vary from 5 to 15 TEC units which correspond to a range error of about 1 to 3 m in the GPS navigation.

3.4.3 Loss of lock of GPS receivers

1. During the equinox months when the occurrence of a strong scintillation is maximum (i.e. $S_4 > 0.45$) around the EIA crest region, it is often found that the GPS receiver loses its lock for a short duration of 1 to 4 min in the phase channel (L1).
2. A multiple number of loss of locks is also observed during some strong scintillation events.
3. During the entire of 18 months period of data considered in the present study, a total of 395 loss of lock events are detected in the Indian sector which are of serious concern for the GPS navigation.
4. The bubble events, as well as the loss of lock events are likely to increase significantly during the high sunspot activity periods, resulting in severe degradation in the trans-ionospheric communications and GPS navigation systems.

Acknowledgements. The research work presented in this paper has been carried out under the Indian Space Research Organization (ISRO, Government of India) sponsored project. The authors are grateful to K. Bandopadhyay and M. R. Sivaraman, Space Application Centre–ISRO, Ahmedabad for providing the GPS data.

Topical Editor M. Pinnock thanks two referees for their help in evaluating this paper.

References

- Aarons, J., Whitney, H. E., MacKenzie, E., and Basu, S.: Microwave equatorial scintillation intensity during solar maximum, *Radio Sci.*, 16, 939–945, 1981.
- Aarons, J.: Global morphology of ionospheric scintillation, *Proc. IEEE*, 70, 360–378, 1982.
- Aarons, J.: The longitudinal morphology of equatorial F-layer irregularities relevant to their occurrence, *Space Sci. Rev.*, 63, 209–243, 1993.
- Anderson, D. N. and Haerendel, G.: The motion of depleted plasma regions in the equatorial ionosphere, *J. Geophys. Res.*, 84, 4251–4256, 1979.
- Basu, S., Kudeki, E., Basu, Su., et al.: Scintillations, plasma drifts, and neutral winds in the equatorial ionosphere after sunset, *J. Geophys. Res.*, 101, 26 795–26 809, 1996.
- Basu, S., MacKenzie, E., and Basu, Su.: Ionospheric Constraints on VHF/UHF Communications Links During Solar Maximum and Minimum Periods, *Radio Science*, 23, 363–378, 1988.
- Conker, R. S., El-Arini, M. B., Hegarty, C. J., and Hsiao, T.: Modeling the effects of ionospheric scintillation on GPS/Satellite Based Augmentation System Availability, *Radio Science*, 38, doi:10.1029/2000RS002604, 1–23, 2003.
- Costa, E. and Kelley, M. C.: On the role of steepened structures and drift waves in equatorial spread F, *J. Geophys. Res.*, 83, 4359–4364, 1978.
- DasGupta, A., Aarons, Basu, S., J., Klobuchar, J. A., Basu, Su., and Bushby, A.: VHF amplitude scintillations and associated electron content depletions as observed at Arequipa, Peru, *J. Atmos. Terr. Phys.*, 45, 15–26, 1983.
- Doherty, P. H., Susan, H. D., and Valladares, C. E.: Ionospheric scintillation effects on GPS in the equatorial and Auroral regions, *Journal of the Institute of Navigation*, Vol. 50, No. 4, 235–245, 2004.
- Eccles, J. V.: Modeling investigation of the evening prereversal enhancement of the zonal electric field in the equatorial ionosphere, *J. Geophys. Res.*, 103, 26 709–26 720, 1998.
- Fejer, B. G., Scherliess, L., and de Paula, E. R.: Effects of the vertical plasma drift velocity on the generation and evolution of equatorial spread F, *J. Geophys. Res.*, 104, 19 859–19 869, 1999.
- Haerendel, G. and Eccles, J. V.: The role of the equatorial electrojet in the evening ionosphere, *J. Geophys. Res.*, 97, 1181–1192, 1992.
- Huang, C. Y., Burke, W. J., Machuzak, J. S., Gentile, L. C., and Sultan, P. J.: DMSP observations of equatorial plasma bubbles in the topside ionosphere near solar maximum, *J. Geophys. Res.*, 106, 8131–8142, 2001.
- Huang, C. S. and Kelly, M. C.: Nonlinear evolution of equatorial spread-F. Gravity wave seeding of Rayleigh Taylor instability, *J. Geophys. Res.*, 101, 293–302, 1996.
- Hysell, D. L. and Burcham, J. D.: JULIA radar studies of equatorial spread F, *J. Geophys. Res.*, 103, 29 155–29 167, 1998.
- Hysell, D. L.: An overview and synthesis of plasma irregularities in equatorial spread F, *J. of Atmos. and Solar-Terrestrial Physics*, 60, 1037–1056, 2000.
- Kelley, M.C., LaBelle, J., Kudeki, E., Fejer, B. G., Basu, S., Basu, Su., Baker, K. D., Hanuise, C., Argo, P., Woodman, R. F., Swartz, W. E., Farley, D. T., and Meriwether, J.: The Condor equatorial spread F campaign: overview and results of the large scale measurements, *J. Geophys. Res.*, 91, 5487–5503, 1986.
- Kelley, M. C., Larson, M. F., LaHoz, C., and McClure, J. P.: Gravity wave initiation of equatorial spread-F: A case study, *J. Geophys. Res.*, 86, 9087–9100, 1981.
- Kelly, M. C.: The Earth's Ionosphere: Plasma physics and electrodynamics, *International Geophysics Series*, vol. 43, Academic Press, San Diego, 1989.
- Kintner, P. M., Kil, H., Beach, T. L., and de Paula, E. R.: Fading Timescales Associated with GPS signals and potential consequences, *Radio Science*, 36, 731–743, 2001.
- Klobuchar, J. A., Anderson, D. N., and Doherty, P. H.: Model studies of the latitudinal extent of the equatorial anomaly during equinoctial conditions, *Radio Science*, 26, 1025–1047, 1991.
- Klobuchar, J. A., Basu, S. and Doherty, P.: Potential limitations in making absolute ionospheric measurements using dual frequency radio waves from GPS satellites, *Proc. of Ionospheric Effects Symposium, IES-93*, May, 187–194, 1993.
- Knight, M. and Finn, A.: The effects of ionospheric scintillation on GPS, *Proceedings of The institute of Navigation's ION GPS-98*,

- Nashville, TN, September 15–18, 673–86, 1998.
- Knight, M., Cervera, M., and Finn, A.: A comparison of predicted and measured GPS performance in an ionospheric scintillation environment, Proceedings of the ION GPS-99, Nashville, Tennessee, September, 1999.
- Leick, A.: GPS Satellite Surveying, second edition, JohnWiley & Sons, USA., 1995.
- Rama Rao, P. V. S., Tulasi Ram, S., Gopi Krishna, S., Niranjana, K., and Prasad, D. S. V. D.: Morphological and Spectral Characteristics of L-band and VHF scintillations and their impact on trans-ionospheric communications, Journal of Earth Planets and Science, in press, 2006.
- Skone, S. and de Jong, M.: The impact of geomagnetic substorms on GPS receiver performance, Earth, Planetary and Space Sciences, 52, 1067–1071, 2000.
- Tsunoda R. T.: Control of the seasonal and longitudinal occurrence of equatorial scintillations by longitudinal gradient in the integrated E-region Pederson conductivity, J. Geophys. Res., 90, 447–456, 1985.
- Van Dierendonck, A. J., Fenton, P., and Klobuchar, J.: Commercial ionospheric scintillation monitoring receiver development and test results, Proceedings of the Institute of Navigation's 52nd Annual Technical Meeting, Cambridge, MA, 573–582, 1996.
- Wanninger, L.: Effects of the Equatorial Ionosphere on GPS, GPS World, 48, 1993.
- Warnant, R.: Reliability of the TEC computed using the GPS measurements: the problem of hardware biases, Acta Geodaetica et Geophysica Hungarica, 32(3–4), 451–459, 1997.
- Woodman, R. F. and LaHoz, C.: Radar observations of F-region equatorial irregularities, J. Geophys. Res., 81, 5 447–5466, 1976.
- Yeh, K. C., Liu, C. H., Soicher, H., and Bonelli, E.: Ionospheric bubbles observed by the Faraday rotation method at Natal, Brazil, Geophys. Res. Lett., 6, 473–475, 1979.